Optimal Synergetic and Feedback Linearization Controllers Design for Magnetic Levitation Systems: A Comparative Study

Fatin R. Al-Ani [1*], Omar F. Lutfy [2], Huthaifa Al-Khazraji [3]
[1, 2, 3] Control and Systems Engineering Department, University of Technology-Iraq, Baghdad 10066, Iraq
Email: [1] cse.22.15@grad.uotechnology.edu.iq, [2] omar.f.lutfy@uotechnology.edu.iq, [3] 60141@uotechnology.edu.iq
*Corresponding Author

***Abstract*—In this paper, the stabilization and trajectory tracking of the magnetic levitation (Maglev) system using optimal nonlinear controllers are investigated. Firstly, the overall structure and physical principle represented by the nonlinear differential equations of the Maglev system are established. Then, two nonlinear controllers, namely synergetic control (SC) and feedback linearization based state feedback controller (FL-SFC), are proposed to force the ball's position using the voltage control input in the Maglev system to track a desired trajectory. For the SC design, the Lyapunov function is employed to guarantee an exponential convergence of the tracking error to zero. In the FL-SFC approach, an equivalent transformation is used to convert the nonlinear system into a linear form, and then the state feedback controller (SFC) method is utilized to track the ball to the desired position. The swarm bipolar algorithm (SBA) based on the integral time absolute error (ITAE) cost function is employed to determine the gains of the controllers to achieve the desired response. Computer simulations are conducted to evaluate the performance of the proposed methodology. The results indicate that in normal conditions, the SC controller is more effective than the FL-SFC controller in controlling the Maglev system. Both controllers achieve zero maximum overshoot and zero steady-state error, but SC responds faster, with a settling time of 0.35 seconds compared to FL-SFC's 1.2 seconds. This highlights SC's superior dynamic performance in speed and accuracy. Additionally, when the Maglev system experiences external disturbances, SC shows better resilience, recovering in just 0.1 seconds, while FL-SFC takes 0.65 seconds. The SC exhibits better performance than that of the FL-SFC in terms of reducing the ITAE index and improving the transient response, even when external disturbances are applied.**

***Keywords*—Magnetic Levitation System; Nonlinear Control; Synergetic Control; Lyapunov Function; Feedback Linearization; State Feedback Controller; Swarm Bipolar Algorithm.**

I. INTRODUCTION

Magnetic levitation (Maglev) systems have numerous industrial applications because of their contactless and frictionless properties that increase efficiency and reduce mechanical wear out and maintenance costs [1]-[6]. Specifically, the system consists of a ferromagnetic ball with a specific amount of mass. The object is suspended in the air gap using the force exerted by the magnetic field whose strength can be controlled through the applied voltage [7]-[10]. Due to its inherent nonlinearities and highly unstable nature, designing a control algorithm that can maintain stable control of the Maglev system is challenging. In this context, many linear and nonlinear controllers have been proposed to stabilize the system.

For instance, Vinodh Kumar and Jerome [6] developed a method for stabilizing and tracking trajectories in a magnetic levitation system using a PID controller. The PID controller gains were determined using the Linear Quadratic Regulator (LQR) approach. First, a nonlinear mathematical model of the system was obtained from first principles around the equilibrium point to implement the stabilizing controller. Then, the PID controller gains were determined to achieve the desired response using the LQR theory. Based on the closed-loop system's natural frequency and damping ratio, a new criterion for selecting the LQR weighting matrices was proposed. Ahmad et al. [11] developed a Proportional-Integral-Derivative (PID) controller for the Maglev system. To optimize the performance indices, the tuning parameters of the PID controller were adjusted using the Genetic Algorithm (GA). When compared to the traditional Ziegler-Nichols (ZN) tuning method, the simulation results indicated that the GA-tuned PID controller outperformed the PID controller tuned by the conventional ZN approach.

Benomair et al. [12] suggests an optimal linear quadratic regulator by utilizing an enhanced spiral dynamic algorithm for the active control of a magnetic levitation system with full-state feedback linearization. Simulations conducted using the nonlinear mathematical model of the magnetic levitation system demonstrate that the proposed linearization and control approach yield effective results. Roy et al. [13] conducted a comparative study of the FOPID controller and the classical PID controller for controlling the position of the ball in the Maglev system. They employed three swarm optimization algorithms: The Gravitational Search Algorithm (GSA), the Particle Swarm Optimization (PSO), and a hybrid algorithm of both methods, called the PSOGSA, to tune the controller parameters. The results, based on a variety of test signals, demonstrated that the hybrid PSOGSA algorithm outperformed the standalone algorithms. Additionally, the FOPID controller exhibited improved performance compared to the PID controller. In addition, Ataşlar-Ayyildiz and Karahan [14] introduced a robust PID-type fuzzy logic controller (Fuzzy-PID) to enhance the system dynamics and stability of the Maglev system. They proposed using the Cuckoo Search (CS)

algorithm to optimize the controller parameters, employing time domain response characteristics as the objective function. Simulation experiments were conducted to evaluate the controller's performance under various conditions, including load disturbances and reference changes. The results demonstrated that the CS-based Fuzzy-PID outperforms traditional FOPID and PID controllers in terms of steady-state error, settling time, overshoot, and control effort requirements. In another work, Ekinci et al. [15] proposed a PID plus second-order derivative (PIDD2) controller for the Maglev system. They utilized a novel metaheuristic algorithm called Manta Ray Foraging Optimization (MRFO), combined with the Generalized Opposition-Based Learning (GOBL) technique and the Nelder–Mead (NM) simplex search method, to optimize the design variables of the proposed controller. Notably, most studies have relied on a linearized model for the controller design. For example, Chiem and Thang [16] introduced a linear feedforward control method combined with a fuzzy logic controller (FLC) for the Maglev system. This proposed controller ensures the stability of the ball and enhances the system's response speed when the ball deviates from its equilibrium position. The performance of this control algorithm was compared to that of conventional PID and standalone FLC controllers. The results indicated a rapid and stable response, even in the presence of noise. However, a limitation of these studies is their reliance on the linear model of the Maglev system. In terms of designing a controller for the nonlinear model of the Maglev system, Al-Muthairi and Zribi [17] proposed a sliding mode control (SMC) to ensure the asymptotic regulation of the Maglev system's states to their desired values. To mitigate the chattering problem, they proposed two modifications of the SMC. The robustness of the developed control schemes to variations in the system parameters was investigated, and it was found that the control schemes are indeed robust to parameter variations. Another application of the SMC to the Maglev system was achieved by Ma'arif et al. [18]. The SMC-controlled system exhibited a fast response with no steady-state error. However, the authors did not provide a solution to the chattering problem in the study. In another work, Uswarman et al. [19] presented a comparative study between the conventional SMC (CSMC) and the SMC with gain-scheduling. The simulation results indicated that the gain-scheduled SMC outperformed the CSMC in terms of resistance to external disturbances. However, both controllers still exhibited the chattering problem. In this regard, a review of the existing literature shows that the SMC has been employed in controller design using the nonlinear model of the Maglev system.

Uswarman et al. [20] demonstrated the application of feedback linearization controller to magnetic levitation. The system's dynamics are examined using the Euler-Lagrange method. The mathematical model reveals that the system is nonlinear. By applying feedback linearization, the original nonlinear system is converted into an equivalent linear system. The controller's performance is tested through MATLAB simulations, which indicate that the controlled output accurately tracks the desired reference. Experiments conducted on a Quanser magnetic levitation system validated the effectiveness of the proposed control strategy in stabilizing the ball and rejecting disturbances in the system. The contributions of this study can be listed as follows:

- Two nonlinear controllers, including the synergetic control (SC) and the feedback linearization-based state feedback controller (FL-SFC), are proposed for the stabilization and trajectory tracking of the Maglev system utilizing the nonlinear model of the system under numerous operations.
- The Lyapunov theory is used for the stability analysis of the proposed controllers.
- The swarm bipolar algorithm is proposed to optimally tune the design parameters of the proposed controllers to improve the dynamic performance of the system.

II. MATHEMATICAL MODEL

The magnetic levitation (Maglev) system consists of a ferromagnetic ball suspended in a voltage-controlled magnetic field [20]. The objective of the Maglev control system is to achieve high accuracy in positioning the small steel ball in a steady position at a stable levitation [21]. The nonlinear nature of magnetic levitation arises from the relationship between the magnetic force and the distance between the levitated object and the magnet. As the distance changes, the magnetic force does not vary linearly. This nonlinearity leads to complex dynamics in the system, making control more challenging, especially when adjusting for position and stability. The schematic of the maglev system is illustrated in Fig. 1 [18]. Specifically, the parameters of the system with their symbols are the electromagnetic force (fe), the gravitational force (fg), the inductance (L), the resistance (R), the object position (x), the source voltage (V), the object mass (m), and the current (i).

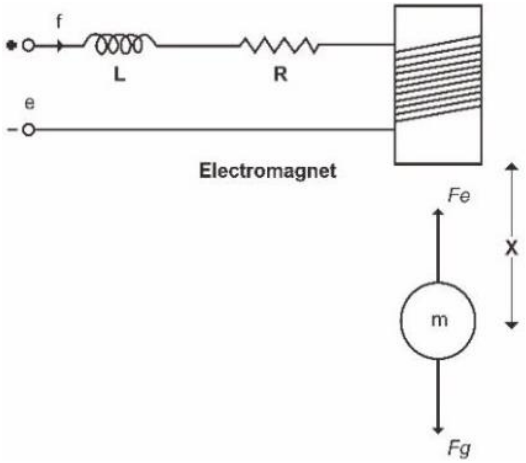

Fig. 1. Maglev system

The dynamics of the Maglev mechanical parts can be expressed based on the second Newton law of motion as follows [10]:

$$m\frac{d^2x}{dt^2} = fg - fe \quad (1)$$

where the electromagnetic force and the gravitational force are expressed as (2) and (3):

$$fg = mg \tag{2}$$

$$fe = \frac{1}{2} i^2 \frac{d}{dx}\big(L(x)\big) \tag{3}$$

The function $L(x)$ is a nonlinear function that can be represented as:

$$L(x) = L + L_0 x_0 \tag{4}$$

Equation (4) can be approximated as [17]:

$$L(x) = \frac{2k}{x^2} \tag{5}$$

where k is the force constant. Substituting Eq. (5) in Eq. (3) gives:

$$fe = k\left(\frac{i}{x}\right)^2 \tag{6}$$

Substituting Eq. (2) and (6) in Eq. (1) gives:

$$m\frac{d^2x}{dt^2} = mg - k\left(\frac{i}{x}\right)^2 \tag{7}$$

By rearranging Eq. (7), we get:

$$\frac{d^2x}{dt^2} = g - \frac{k}{m}\left(\frac{i}{x}\right)^2 \tag{8}$$

Besides the mechanical analysis, the Kirchhoff law of voltage in the electrical system can be used to generate Eq. (9).

$$e = iR + \frac{d}{dt}\, L(x) i \tag{9}$$

Using simple mathematical operations, the equation can be rewritten as:

$$\frac{di}{dt} = -\frac{R}{Li} - \frac{2k}{L}\frac{i}{x^2}\frac{dx}{dt} + \frac{1}{L}e \tag{10}$$

By assuming that the states of the system are $x_1 = x, x_2 = \frac{dx}{dt}, x_3 = i$, and the control input to the system is $u = e$, the nonlinear differential equations that capture the dynamics of the Maglev system can be represented as shown below:

$$\frac{dx_1}{dt} = x_2 \tag{11}$$

$$\frac{dx_2}{dt} = g - \frac{kx_3^2}{mx_1^2} \tag{12}$$

$$\frac{dx_3}{dt} = -\frac{Rx_3}{L} + \frac{2kx_2x_3}{Lx_1^2} + \frac{u}{L} \tag{13}$$

where $x_1 > 0$ and $x_3 > 0$.

The system's output can be described as:

$$y = x_1 \tag{14}$$

In particular, the nonlinearity features are visible in Eq. (12) and Eq. (13), as can be noticed in the dynamics of the Maglev system. To design the controller, the model of the Maglev is transformed into an equivalent canonical form, which is a more straightforward model that exhibits the nonlinearity using only one dynamic equation. The definition of the nonlinear transformation in coordinates is as follows:

$$z_1 = x_1 \tag{15}$$

$$z_2 = x_2 \tag{16}$$

$$z_3 = g - \frac{kx_3^2}{mx_1^2} \tag{17}$$

Thus, the equivalent model in the new coordinates can be expressed as:

$$\dot{z}_1 = z_2 \tag{18}$$

$$\dot{z}_2 = z_3 \tag{19}$$

$$\dot{z}_3 = f(z) + g(z)u \tag{20}$$

Where

$$f(z) = \frac{2kR\, x_3^2}{mx_1^2 L} - \frac{4k^2\, x_3^2 x_2}{mx_1^4 L} + \frac{2kx_2x_3^2}{mx_1^3} \tag{21}$$

$$g(z) = -\frac{2kx_3}{mx_1^2 L} \tag{22}$$

III. CONTROLLER DESIGN

The use of feedback controllers is constantly expanding to control a wide range of systems [23]-[29]. In this context, controlling the Maglev system involves addressing a range of issues, such as tracking control and handling external disturbances. Particularly, this section explores two nonlinear control strategies to generate the control law for the Maglev system, including the synergetic control (SC) and the feedback linearization (FL-SFC). These two nonlinear controllers are well-suited for the Maglev system because they are effectively handles the system's nonlinear dynamics, ensuring rapid and stable positioning of the levitated object while maintaining resilience to disturbances.

A. Synergetic Control

SC is a control technique that can be applied to various dynamical systems, especially for nonlinear dynamical systems, to obtain a stable control model. In particular, synergetic control has been successfully applied to various systems, such as permanent magnet synchronous motor (PMSM) drives and DC micro-grids with constant power loads (CPLs), demonstrating its effectiveness in controlling nonlinear systems with uncertainties [48]:

Let's define e as the error between the actual and the desired outputs:

$$e = z_r - z_1 \tag{23}$$

Taking the derivative of the error gives:

$$\dot{e} = \dot{z}_r - \dot{z}_1 \tag{24}$$

By substituting Eq. (18) in Eq. (24), we get:

$$\dot{e} = \dot{z}_r - z_2 \tag{25}$$

Taking the second derivative of the error gives:

$$\ddot{e} = \ddot{z}_r - \dot{z}_2 \tag{26}$$

Substituting Eq. (19) in Eq. (26) gives (27):

$$\ddot{e} = \dddot{z}_r - z_3 \quad (27)$$

By taking the third derivative of the error, we get:

$$\dddot{e} = \dddot{z}_r - \dot{z}_3 \quad (28)$$

Substituting Eq. (20) in Eq. (28) gives:

$$\dddot{e} = \dddot{z}_r - f(z) - g(z)u \quad (29)$$

Define a macro-variable:

$$\psi = \psi(z)$$

More precisely, the macro-variable ψ is selected as:

$$\psi = c_1 e + c_2 \dot{e} + \ddot{e} \quad (30)$$

Taking the derivative of the macro-variable ψ gives:

$$\dot{\psi} = c_1 \dot{e} + c_2 \ddot{e} + \dddot{e} \quad (31)$$

The desired dynamic evolution of the macro-variable is:

$$\dot{\psi} + c_3 \psi = 0 \quad (32)$$

$$\dot{\psi} = -c_3 \psi \quad (33)$$

Substituting Eq. (31) in Eq. (32) gives:

$$c_1 \dot{e} + c_2 \ddot{e} + \dddot{e} + c_3 \psi = 0 \quad (34)$$

By substituting Eq. (29) in Eq. (34), we obtain:

$$c_1 \dot{e} + c_2 \ddot{e} + \dddot{z}_r - f(z) - g(z)\, u + c_3 \psi = 0 \quad (35)$$

Select u as follows:

$$u_{sc} = \frac{1}{g(z)}(-f(z) + \dddot{z}_r + c_1 \dot{e} + c_2 \ddot{e} + c_3 \psi) \quad (36)$$

Choose the Lyapunov function as:

$$\mathrm{V} = \frac{1}{2}\psi^2 \quad (37)$$

Taking the derivative of V gives:

$$\dot{V} = \psi \dot{\psi} \quad (38)$$

Substitute Eq. (33) in Eq. (38):

$$\dot{V} = \psi (-c_3 \psi) \quad (39)$$

$$\dot{V} = -c_3 \psi^2 \quad (40)$$

B. *Feedback Linearization-based State Feedback Controller*

One of the well-researched strategies for designing trajectory tracking controllers for nonlinear systems is the feedback linearization (FL) approach [32]-[35]. The control law in FL is designed such that the nonlinear system is transformed into an equivalent linear form as follows:

$$u_{fl} = \frac{1}{g(x)}(-f_X + u_l) \quad (41)$$

where u_l can be any linear controller. In this paper, a state feedback controller (SFC) is selected as follows:

$$u_l = k_1(z_r - z_1) - k_2 z_2 - k_3 z_3 \quad (42)$$

where k_1, k_2 and k_3 are the SFC gains that are designed such that the desired tracking performance is achieved.

C. *Swarm Optimization*

Swarm optimization algorithms are essential techniques for solving numerous complex problems [36]-[48]. Unlike the trial-and-error method, in this work, the tuning process of the BSC and the FL design variables is formulated as an optimization problem. Subsequently, the optimization problem is solved by the swarm bipolar algorithm (SBA), which is a recent swarm optimization technique introduced in [49].

In particular, the SBA is a unique method that splits a swarm into two equal sub-swarms (i.e., one-half of the population is allocated to one sub-swarm, while the other half is assigned to the second sub-swarm). During the initialization phase, all swarm members are distributed throughout the search space. Then, the population is divided into two equal sub-groups. This division is random and not based on the positions of the swarm members in the search space, allowing for a mix of individuals from both sub-swarms. Moreover, SBA makes use of four key references: the best swarm member, the best sub-swarm member, the midpoint between the two best sub-swarm members, and a randomly chosen member from the opposite sub-swarm. These references guide the directed search operations carried out by each swarm member in the iteration process [49]. As the swarm progresses towards the best swarm member, the paths are adjusted to converge towards a specific region. With time, the swarm distribution polarizes into two distinct clusters, moving towards the midpoint between the two best sub-swarm members. The illustration of these four search operations is presented in Fig. 2. Algorithm 1 presents the pseudo code that formalizes SBA.

The procedure of the SBA is mathematically formulated using Eq. (53) to Eq. (62). Specifically, Eq. (53) to Eq. (56) are applied at the startup stage. The uniform distribution is utilized to generate the initial solution of the swarm members, as given in Eq. (53). The rigorous acceptance role used to update the best swarm member is represented by Eq. (54). The first-best sub-swarm member is updated using Eq. (55), while the second-best sub-swarm member is updated using Eq. (56) [49].

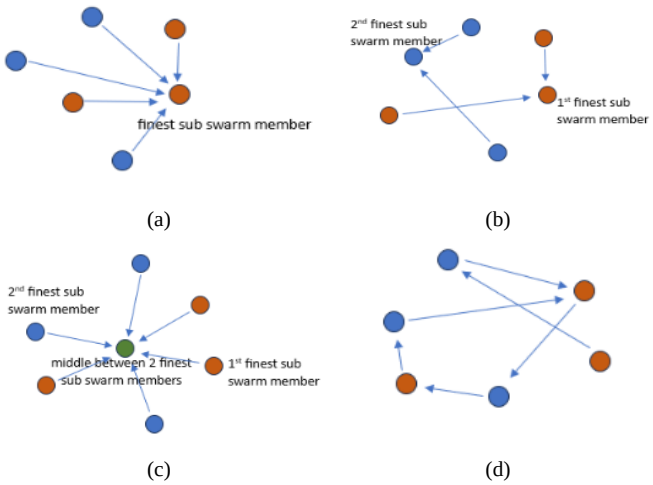

Fig. 2. Illustration of four search operations: (a) first search, (b) second search, (c) third search, and (d) fourth search

Algorithm 1. Pseudo code of SBA

1. **Begin**
2. **For each s ∈ S do**
3. **Generate** the initial solution using Eq. (43)
4. **Update** $s_b$and s_{sb} using Eq. (44) to Eq. (46)
5. **End For**
6. **For** $t = 1$ to t_m do
7. **For each s ∈ S do**
8. **First** search using Eq. (47) and Eq. (48)
9. **Update** $s_b$and s_{sb} using Eq. (44) to Eq. (46)
10. **Second** search using Eq. (49) and Eq. (48)
11. **Update** $s_b$and s_{sb} using Eq. (44) to Eq. (46)
12. **Third** search using Eq. (50) and Eq. (48)
13. **Update** $s_b$and s_{sb} using Eq. (44) to Eq. (46)
14. **Fourth** search using Eq. (51), Eq. (52), Eq. (48)
15. **Update** $s_b$and s_{sb} using Eq. (44) to Eq. (46)
16. **End For**
17. **End For**
18. **Return** s_b
19. **End**

The notations of the SBA are listed below:

d	Dimension
F	objective function
I	index for swarm member
J	index for dimension
S	swarm member
S	swarm/population
s_l	lower boundary
s_u	upper boundary
s_b	the best swarm member
s_{sb}	the best sub swarm member
s_t	randomly picked swarm member
r_1	floating point uniform random [0,1]
r_2	integer uniform random [1,2]
T	Iteration
t_m	maximum iteration
U	uniform random

$$s_{i,j} = s_{l,j} + r_1\left(s_{u,j} - s_{l,j}\right) \tag{43}$$

$$s_b = \begin{Bmatrix} s_i, f(s_i) < f(s_b) \\ s_b, else \end{Bmatrix} \tag{44}$$

$$s_{sb1} = \begin{Bmatrix} s_i, f(s_i) < f(s_{sb1}) \ \wedge 1 \le i \le \frac{n(s)}{2} \\ s_{sb1}, else \end{Bmatrix} \tag{45}$$

$$s_{sb2} = \begin{Bmatrix} s_i, f(s_i) < f(s_{sb2}) \ \wedge \frac{n(s)}{2} < i < n(s) \\ s_{sb2}, else \end{Bmatrix} \tag{46}$$

Equations (47) to (52) present the mathematical equations during the improvement process. The initial search involves finding the best swarm member according to Eq. (47). The rigorous acceptance role in accepting the candidate solution to replace the swarm member's existing value is represented by Eq. (48). The second search's candidate solution is produced by Eq. (49), in which each sub-swarm member travels in the direction of its own best sub-swarm member. In the third search, all swarm members migrate toward the midpoint between the two best sub-swarm members using Eq. (50). Next, the randomly selected swarm member from the opposing sub-swarm is defined by Eq. (51). Subsequently, the fourth search's movement is represented by Eq. (52), which is dependent on the swarm member's quality comparison and its reference [49].

$$c_{i,j} = s_{b,j} + r_1\left(s_{b,j} - r_2 s_{i,j}\right) \tag{47}$$

$$s_i' = \begin{Bmatrix} c_i, f(c_i) < f(s_i) \\ s_i, else \end{Bmatrix} \tag{48}$$

$$c_{i,j} = \begin{Bmatrix} s_{i,j} + r_1\left(s_{sb1,j} - r_2 s_{i,j}\right), \wedge 1 \le i \le \frac{n(s)}{2} \\ s_{i,j} + r_1\left(s_{sb2,j} - r_2 s_{i,j}\right), \wedge \frac{n(s)}{2} < i < n(S) \end{Bmatrix} \tag{49}$$

$$c_{i,j} = s_{b,j} + r_1\left(\frac{s_{sb1,j} + s_{sb2,j}}{2} - r_2 s_{i,j}\right) \tag{50}$$

$$s_t = \begin{Bmatrix} U\left(s_1, \frac{s_{n(s)}}{2}\right), \frac{n(s)}{2} < i < n(S) \\ U\left(s_1, \frac{s_{n(s)}}{2}\right), 1 \le i \le \frac{n(s)}{2} \end{Bmatrix} \tag{51}$$

$$c_{i,j} = \begin{Bmatrix} s_{i,j} + r_1\left(s_{t,j} - r_2 s_{i,j}\right), f(s_t) < f(s_i) \\ s_{i,j} + r_1\left(s_{i,j} - r_2 s_{t,j}\right), else \end{Bmatrix} \tag{52}$$

IV. SIMULATION RESUTS

In this section, computer simulations are carried out to evaluate the effectiveness of the proposed control strategy. The results are further analysed to assess their comparative performance.

A. Simulation Setup

The simulation process of the Maglev system with SC and FL-SFC has been conducted using Matlab software. The parameters of the Maglev system are given in Table I [18]. The configurations of the SC and FL-SFC controllers based SBA which is applied to the Maglev system are shown in Fig. 3 and Fig. 4. The initial position of the ball was set to 1 mm, and the desired position was 5 cm.

TABLE I. PARAMETERS OF THE MAGLEV SYSTEM

Parameters	Values
Mass (m)	0.0221 Kg
Inductance (L)	0.02 H
Resistance (R)	4.2 Ω
Force constant (k)	8.25×10^-5 Nm2/A2
Gravity acceleration (g)	9.81 m/s2

To ensure the best performance of each controller, the SBA is employed to tune the design parameters of each controller. The performances of the SC and the FL-SFC are optimized by tuning the adjustable parameters (c_1, c_2, and c_3) and (k_1, k_2, and k_3) of the control laws given in Eq. (36) and Eq. (52), respectively.

The Integral Time of Absolute Errors (ITAE) is used as a cost function to tune the performance of the two controllers, as given in Eq. (53) [50]-[53].

$$ITAE = \int_{t=0}^{t=t_{sim}} tt|e(t)|dt \tag{53}$$

Where t_{sim} refers to the total simulation time. The parameters of the SBA are selected as given in Table II.

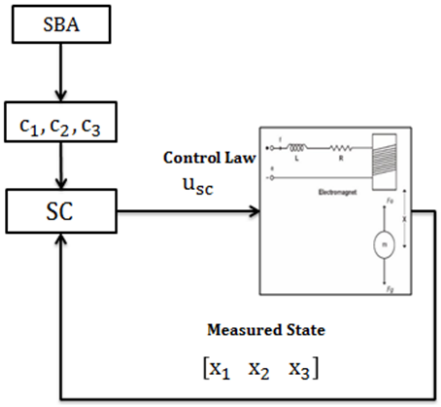

Fig. 3. Proposed SC controller tuned by SBA

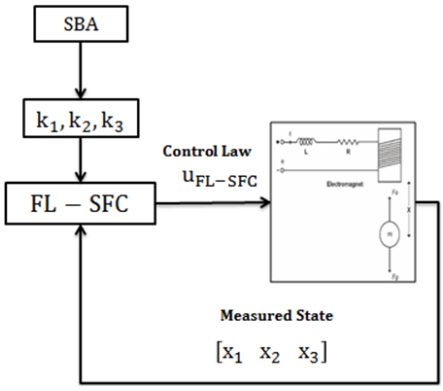

Fig. 4. Proposed FL-SFC controller tuned by SBA

TABLE II. ALGORITHM PARAMETERS OF SBA

Parameters	Values
Population Size (N)	25
Number of Iterations (T_{max})	40

The convergence behavior of the cost function based on SBA algorithm to find the design variables of the SC and the FL-SFC is illustrated in Fig. 5 and the design variables are listed in Table III.

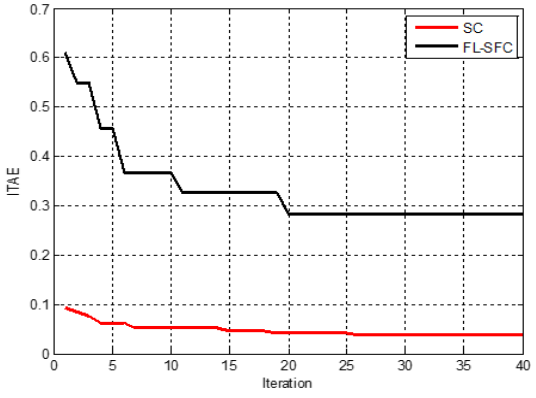

Fig. 5. SBA' convergence

TABLE III. OPTIMAL SETTING OF THE CONTROLLERS

Controller	Parameter	Value
SC	c_1	125
	c_2	20
	c_3	75
FL-SFC	k_1	80
	k_2	50
	k_3	12

B. *Evaluation in Normal Conditions*

Fig. 6 depicts the responses of the Maglev system to the step input. The corresponding control signals generated by the proposed controllers are illustrated in Fig. 7. By comparing the two control approaches (SC and FL-SFC), as shown in Fig. 6 and the numerical result in Table 4, it can be observed that the two controllers are effectively able to control the Maglev system with zero maximum overshoot (Mo) and zero error steady state ($e_{s.s}$).

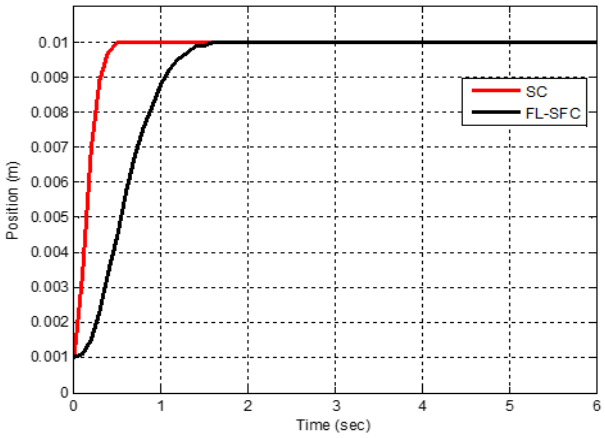

Fig. 6. Position's response of Maglev

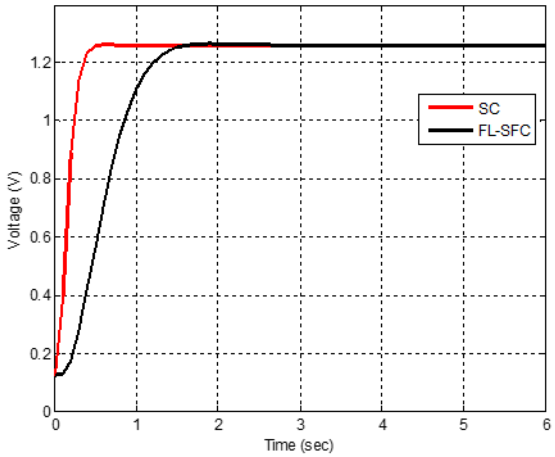

Fig. 7. Control signals

The results also show that the SC has a faster tracking response to the desired output than the FL-SFC where the settling time (t_s) is reduced from 1.2s for the FL-SFC to 0.35s for the SC. Moreover, the SC achieves an 86.7% improvement in ITAE over FL-SFC, demonstrating its superior tracking ability under normal conditions, where the ITAE index is reduced from 0.2827 for the FL-SFC to 0.0374 for the SC. Besides, Fig. 7 shows that there is no chattering in the control law of the two controllers.

C. *Evaluation under External Disturbance*

The rejection of the external disturbance of the SC and the FL-SFC is evaluated by applying an external disturbance to each controlled system after 15 sec of the simulation Fig. 8 shows the response of the two controlled systems under disturbance. The recovery time (t_r) and the maximum undershoot (Mu) are used to evaluate the two controllers. The dynamic responses of the two controllers with disturbance are reported in Table IV.

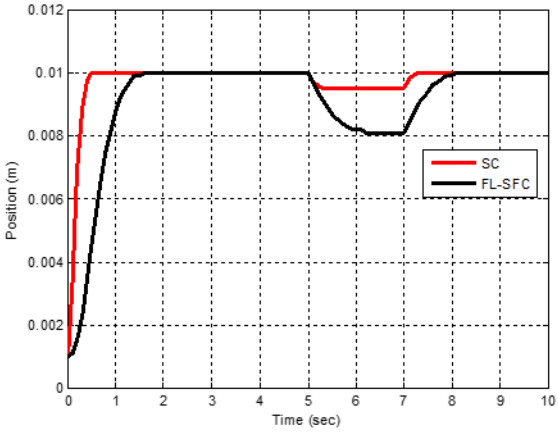

Fig. 8. Position's response of Maglev under external disturbance

TABLE IV. SYSTEM'S PERFORMANCES

Controller	$t_s(s)$	$e_{s.s}(rad)$	$Mo(\%)$	ITAE
SC	0.35	0	0	0.0374
FL-SFC	1.2	0	0	0.2827

In this context, it is clear from Fig. 8 and Table V that the ball's position is recovered from the disturbance to the desired position and remained stable for both controllers. However, SC has better disturbance rejection where M_u of the SC was 5 and 19 for FL-SFC. Besides, t_r was 0.1 for the SC which is less as compared to 0.65of the FL-SFC.

The aforementioned simulation results demonstrate that the SC is capable of effectively controlling the Maglev system in a better manner compared to the FL-SFC for the two studied scenarios. These scenarios include the normal operation and the influence of external disturbances.

TABLE V. SYSTEM'S PERFORMANCES UNDER EXTERNAL DISTURBANCE

Controller	$t_r(s)$	$Mu(\%)$
SC	0.1	5
FL-SFC	0.65	19

D. Comparison with Published Work

For the purpose of comparison with published paper, result of the SC is compared with the result that is presented in [12]. The comparison result is given in Table VI. The comparison shows that the SC has achieved a faster tracking response to the desired output than that of the controller of [12] where t_s is reduced from 0.52 for [12] to 0.35 for the SC.

TABLE VI. SC'S PERFORMANCE COMPARISON WITH PUBLISHED WORK

Controller	$t_s(s)$	$e_{s.s}(rad)$	$Mo(\%)$
SC	0.35	0	0
Ref. [12]	0.52	0	0

V. CONCLUSION

This paper presented the design and optimization of SC and FL-SFC controllers for the Maglev system, using the Swarm Bipolar Algorithm (SBA) to avoid the limitations of manual parameter tuning. To demonstrate the effectiveness of the synthesized controllers, a numerical comparative simulation based on MATLAB was performed. The comparative analysis demonstrates that SC consistently outperforms FL-SFC in both normal operation and disturbance scenarios, offering superior dynamic response, control precision, and resilience. The results showed under normal operation, the findings demonstrate that SC outperforms FL-SFC in controlling the Maglev system. Both controllers successfully maintain successfully maintain zero maximum overshoot and zero steady-state error. However, SC exhibits the fastest tracking response to the desired output, with a settling time reduced to 0.35 seconds, compared to 1.2 seconds for FL-SFC. These results underscore SC's superior dynamic performance, particularly in terms of response speed and control precision, relative to the other methods. When the Maglev system is subjected to an external disturbance, the findings demonstrate that SC outperforms FL-SFC. SC exhibits better resilience response with a recovery time reduced to 0.1 seconds, compared to 0.65 seconds for FL-SFC.

The improved settling time and disturbance rejection capability of SC make it suitable for high-precision applications, such as transportation systems or magnetic bearings, where quick stabilization is crucial. Future research could explore the performance of SC in more complex scenarios, such as non-linear disturbances or parameter variations, and investigate its implementation on real hardware for practical validation. Besides, another swarm optimization as African vultures' optimization algorithm [54] could be used to select the design parameters of the controllers. Another extension of this study could be by applying a hybrid nonlinear controller such as backstepping sliding mode control [55]-[56] for the Maglev system. Moreover, the limitation of the present work is by assumed that all the states of the system are measured. Hence, observer [57]-[60] can be applied to overcome this limitation in the future

REFERENCES

[1] A. Bizuneh, H. Mitiku, A. O. Salau, and K. Chandran, "Performance analysis of an optimized PID-P controller for the position control of a magnetic levitation system using recent optimization algorithms," *Measurement Sensors*, vol. 33, p. 101228, 2024.

[2] K. Hu, H. Jiang, Q. Zhu, W. Qian, and J. Yang, "Magnetic levitation belt conveyor control system based on multi-sensor fusion," *Applied Sciences*, vol. 13, no. 13, p. 7513, 2023.

[3] P. Kumar, M. Ansari, E. Toyserkani, and M. B. Khamesee, "Experimental implementation of a magnetic levitation system for laser-directed energy deposition via powder feeding additive manufacturing applications," *Actuators*, vol. 12, no. 6, p. 244, 2023.

[4] S. Ge, A. Nemiroski, K. A. Mirica, C. R. Mace, J. W. Hennek, A. A. Kumar and G. M. Whitesides, "Magnetic levitation in chemistry, materials science, and biochemistry," *Angewandte Chemie International Edition*, vol. 59, no. 41, pp. 17810-17855, 2020.

[5] R. S. Gopi, S. Srinivasan, K. Panneerselvam, Y. Teekaraman, R. Kuppusamy and S. Urooj, "Enhanced Model Reference Adaptive Control Scheme for Tracking Control of Magnetic Levitation System," *Energies*, vol. 14, no. 5, p. 1455, 2021.

[6] E. V. Kumar and J. Jerome, "LQR based optimal tuning of PID controller for trajectory tracking of magnetic levitation system," *Procedia Engineering*, vol. 64, pp. 254-264, 2013.

[7] P. Majewski, D. Pawuś, K. Szurpicki, and W. P. Hunek, "Toward optimal control of a multivariable magnetic levitation system," *Applied Sciences*, vol. 12, no. 2, p. 674, 2022.

[8] W. Bauer and J. Baranowski, "Fractional PI λ D controller design for a magnetic levitation system," *Electronics*, vol. 9, no. 12, p. 2135, 2020.

[9] S. Dey, J. Dey, and S. Banerjee, “Optimization algorithm based PID controller design for a magnetic levitation system,” in *2020 IEEE Calcutta Conference (CALCON)*, pp. 258-262, 2020.

[10] A. Abbas, S. Z. Hassan, T. Murtaza, A. Mughees, T. Kamal, M. A. Khan, and Q. D. Memon, “Design and control of magnetic levitation system,” *2019 International Conference on Electrical, Communication, and Computer Engineering (ICECCE)*, pp. 1-5, 2019.

[11] I. Ahmad, M. Shahzad, and P. Palensky, “Optimal PID control of magnetic levitation system using genetic algorithm,” in *2014 IEEE Internationa lEnergy Conference (ENERGYCON)*, pp. 1429-1433, 2014.

[12] A. M. Benomair, F. A. Bashir, and M. O. Tokhi, "Optimal control based LQR-feedback linearisation for magnetic levitation using improved spiral dynamic algorithm," *2015 20th International Conference on Methods and Models in Automation and Robotics (MMAR)*, pp. 558-562, 2015.

[13] P. Roy, M. Borah, L. Majhi, and N. Singh, “Design and implementation of FOPID controllers by PSO, GSA and PSOGSA for MagLev system,” in *2015 International Symposium on Advanced Computing and Communication (ISACC)*, pp. 10-15, 2015.

[14] B. Ataşlar-Ayyildiz and O. Karahan, “Trajectory tracking for the magnetic ball levitation system via fuzzy PID control based on CS algorithm,” in *2019 IEEE International Symposium on INnovations in Intelligent SysTems and Applications (INISTA)*, pp. 1-6, 2019.

[15] S. Ekinci, D. Izci, and M. Kayri, “An effective controller design approach for magnetic levitation system using novel improved manta ray foraging optimization,” *Arabian Journal for Science and Engineering*, vol. 47, no. 8, pp. 9673-9694, 2022.

[16] N. X. Chiem and L. T Thang, “Synthesis of Hybrid Fuzzy Logic Law for Stable Control of Magnetic Levitation System,” *Journal of Robotics and Control (JRC)*, vol. 4, no. 2, pp. 141-148, 2023.

[17] N. F. Al-Muthairi and M. Zribi, “Sliding mode control of a magnetic levitation system,” *Mathematical problem in engineering*, vol. 2004, no. 2, pp. 93-107, 2004.

[18] A. Ma’arif, M. Antonio, M. Sadek, E. Umoh, A. Abougarair, and R. Nurindra, “Sliding Mode Control Design for Magnetic Levitation System,” *Journal of Robotics and Control (JRC)*, vol. 3, no. 6, pp. 848-853, 2022.

[19] R. Uswarman, S. Istiqphara, and D. H. T. Nugroho, “Sliding mode control with gain scheduled for magnetic levitation system,” *Jurnal Ilmiah Teknik Elektro Komputer dan Informatika*, vol. 5, no. 1, pp. 36-43, 2019.

[20] R. Uswarman, A. I. Cahyadi, and O. Wahyunggoro, "Control of a magnetic levitation system using feedback linearization," *2013 International Conference on Computer, Control, Informatics and Its Applications (IC3INA)*, pp. 95-98, 2013.

[21] I. Ahmad and M. A. Javaid, “Nonlinear model & controller design for magnetic levitation system,” *Recent advances in signal processing, robotics and automation*, pp. 324-328, 2010.

[22] S. A. Al-Samarraie, I. I. Gorial, and M. H. Mshari, “An integral sliding mode control for the magnetic levitation system based on backstepping approach,” in *IOP Conference Series: Materials Science and Engineering*, vol. 881, no. 1, p. 012136, 2020.

[23] R. A. Kadhim, M. Q. Kadhim, H. Al-Khazraji, and A. J. Humaidi, “Bee Algorithm Based Control Design for Two-links Robot Arm Systems,” *IIUM Engineering Journal*, vol. 25, no. 2, pp. 367-380, 2024.

[24] R. M. Naji, H. Dulaimi, and H. Al-Khazraji, "An Optimized PID Controller Using Enhanced Bat Algorithm in Drilling Processes," *Journal Européen des Systèmes Automatisés*, vol. 57, no. 3, pp. 767-772, 2024.

[25] M. A. Al-Ali, O. F. Lutfy, and H. Al-Khazraj, “Investigation of Optimal Controllers on Dynamics Performance of Nonlinear Active Suspension Systems with Actuator Saturation,” *Journal of Robotics and Control (JRC)*, vol. 5, no. 4, pp. 1041-1049, 2024.

[26] A. K. Ahmed and H. Al-Khazraji, “Optimal Control Design for Propeller Pendulum Systems Using Gorilla Troops Optimization,” *Journal Européen des Systèmes Automatisés*, vol. 56, no. 4, pp. 575-582, 2023.

[27] Z. N. Mahmood, H. Al-Khazraji, and S. M. Mahdi, "PID-based enhanced flower pollination algorithm controller for drilling process in a composite material," in *Annales de Chimie. Science des Materiaux*, vol. 47, no. 2, pp. 91-96, 2023.

[28] H. Al-Khazraji, C. Cole, and W. Guo, "Dynamics analysis of a production-inventory control system with two pipelines feedback," *Kybernetes*, vol. 46, no. 10, pp. 1632-1653, 2017.

[29] H. Al-Khazraji, C. Cole, and W. Guo, "Analysing the impact of different classical controller strategies on the dynamics performance of production-inventory systems using state space approach," *Journal of Modelling in Management*, vol. 13, no. 1, pp. 211-235, 2018.

[30] E. Oumaymah, O. Abdellah, B. Omar, and E. B. Lhoussain, "Backstepping Design Control Applied to the Wind PMSG Generator and Grid Connection Using A Multilevel Inverter," *2021 8th International Conference on Electrical and Electronics Engineering (ICEEE)*, pp. 136-141, 2021.

[31] M. T. Vo, M. T. Nguyen, T. T. H. Le, V. Do Tran, D. T. Tran, T. M. N. Nguyen, and V. T. Ngo, "Back-stepping control for rotary inverted pendulum," *Journal of Technical Education Science*, vol. 15, no. 4, pp. 93-101, 2020.

[32] H. Al-Khazraji, R. M. Naji, and M. K. Khashan "Optimization of Sliding Mode and Back-Stepping Controllers for AMB Systems Using Gorilla Troops Algorithm," *Journal Européen des Systèmes Automatisés*, vol. 57, no. 2, pp. 417–424, 2024.

[33] M. S, Xavier, A. J. Fleming, and Y. K. Yong, “Nonlinear estimation and control of bending soft pneumatic actuators using feedback linearization and UKF,” *IEEE/ASME Transactions on Mechatronics*, vol. 27, no. 4, pp. 1919-1927, 2022.

[34] M. Vesović, R. Jovanović, and N. Trišović, “Control of a DC motor using feedback linearization and gray wolf optimization algorithm,” *Advances in Mechanical Engineering*, vol. 14, no. 3, 2022.

[35] A. Hache, M. Thieffry, M. Yagoubi, and P. Chevrel, “Control-Oriented Neural State-Space Models for State-Feedback Linearization and Pole Placement,” in *2022 10th International Conference on Systems and Control (ICSC)*, pp. 429-434, 2022.

[36] H. Li, Z. Wang, Z. Xu, X. Wang, and Y. Hu, “Feedback linearization based direct torque control for IPMSMs,” *IEEE Transactions on Power Electronics*, vol. 36, no. 3, pp. 3135-3148, 2020.

[37] H. Al-Khazraji, C. Cole, and W. Guo, "Multi-objective particle swarm optimisation approach for production-inventory control systems," *Journal of Modelling in Management*, vol. 13, no. 4, pp. 1037-1056, 2018.

[38] A. K. Ahmed, H. Al-Khazraji, and S. M. Raafat, “Optimized PI-PD Control for Varying Time Delay Systems Based on Modified Smith Predictor,” *International Journal of Intelligent Engineering & Systems*, vol. 17, no. 1, pp. 331-342, 2024.

[39] H. A. Azzawi, N. M. Ameen, and S. A. Gitaffa, “Comparative Performance Evaluation of Swarm Intelligence-Based FOPID Controllers for PMSM Speed Control,” *Journal Européen des Systèmes Automatisés*, vol. 56, no. 3, pp. 475-482, 2023.

[40] X. Zhao, R. Ogawa, and S. C. Sung, “On Searching Optimal Worker Assignment in Multi-stage Production Lines,” in *The International Conference on Smart Manufacturing, Industrial & Logistics Engineering (SMILE)*, pp. 205-211, 2023.

[41] H. Al-Khazraji, “Optimal Design of a Proportional-Derivative State Feedback Controller Based on Meta-Heuristic Optimization for a Quarter Car Suspension System,” *Mathematical Modelling of Engineering Problems*, vol. 9, no. 2, pp. 575-582, 2022.

[42] H. Al-Khazraji, A.R. Nasser, and S. Khlil, “An intelligent demand forecasting model using a hybrid of metaheuristic optimization and deep learning algorithm for predicting concrete block production,” *IAES International Journal of Artificial Intelligence*, vol. 11, no. 2, pp. 649-657, 2022.

[43] H. Al-Khazraji, W. Guo, and A. J. Humaidi, “Improved Cuckoo Search Optimization for Production Inventory Control Systems,” *Serbian Journal Of Electrical Engineering*, vol. 21, no. 2, pp. 187-200, 2024.

[44] H. AL-Khazraji, C. Cole, and W. Guo, “Optimization and simulation of dynamic performance of production–inventory systems with multivariable controls,” *Mathematics*, vol. 9, no. 5, 2021.

[45] H. Al-Khazraji, S. Khlil and Z. Alabacy, “Industrial picking and packing problem: Logistic management for products expedition,” *Journal of Mechanical Engineering Research and Developments*, vol. 43, no. 2, pp. 74-80, 2020.

[46] P. D. Kusuma and A. Dinimaharawati, "Swarm Bipolar Algorithm: A Metaheuristic Based on Polarization of Two Equal Size Sub Swarms," *International Journal of Intelligent Engineering & Systems*, vol. 17, no. 2, 2024.

[47] M. A. AL-Ali, O. F. Lutfy, and H. Al-Khazraj, "Comparative Study of Various Controllers Improved by Swarm Optimization for Nonlinear Active Suspension Systems with Actuator Saturation," *International Journal of Intelligent Engineering & Systems*, vol. 17, no. 4, pp. 870-881, 2024.

[48] Z. N. Mahmood, H. Al-Khazraji, and S. M. Mahdi, "Adaptive control and enhanced algorithm for efficient drilling in composite materials," *Journal Européen des Systèmes Automatisés*, vol. 56, no. 3, pp. 507-512, 2023.

[49] O. T. Altinoz and A. E. Yilmaz, "Optimal PID design for control of active car suspension system," *International Journal of Information Technology and Computer Science (IJITCS)*, vol. 10, no. 1, pp. 16-23, 2018.

[50] A. Wireko-Brobby, Y. Hu, G. Wang, C. Gong, W. Lang, and Z. Zhang, "Analysis of the Sources of Error Within PMSM-Based Electric Powertrains—A Review," in *IEEE Transactions on Transportation Electrification*, vol. 10, no. 3, pp. 6370-6406, Sept. 2024.

[51] R. Zaheer and H. Shaziya, "A Study of the Optimization Algorithms in Deep Learning," *2019 Third International Conference on Inventive Systems and Control (ICISC)*, pp. 536-539, 2019.

[52] J. F. Okulicz *et al*., "Clinical outcomes of elite controllers, viremic controllers, and long-term nonprogressors in the US Department of Defense HIV natural history study," *The Journal of infectious diseases*, vol. 200, no. 11, pp. 1714-1723, 2009.

[53] S. R. Gampa, S. K. Mangipudi, K. Jasthi, P. Goli, D. Das, and V. Balas, "Pareto optimality based PID controller design for vehicle active suspension system using grasshopper optimization algorithm," *Journal of Electrical Systems and Information Technology*, vol. 9, no. 1, p. 24, 2022.

[54] M. S. Abed, O. F. Lutfy, and Q. F. Al-Doori, "Online path planning of mobile robots based on African vultures optimization algorithm in unknown environments," *Journal Européen des Systèmes Automatisés*, vol. 55, no. 3, pp. 405-412, 2022.

[55] A. Ma'arif, M. A. M. Vera, M. S. Mahmoud, S. Ladaci, A. Çakan, and J. N. Parada, "Backstepping sliding mode control for inverted pendulum system with disturbance and parameter uncertainty," *Journal of Robotics and Control (JRC)*, vol. 3, no. 1, pp. 86-92, 2022.

[56] F. E. Z. Lamzouri, E. M. Boufounas, M. Hanine, and A. E. Amrani, "Optimised backstepping sliding mode controller with integral action for MPPT-based photovoltaic system using PSO technique," *International Journal of Computer Aided Engineering and Technology*, vol. 18, pp. 97-109, 2023.

[57] N. S. Mahmood, A. J. Humaidi, R. S. Al-Azzawi, and A. Al-Jodah, "Extended state observer design for uncertainty estimation in electronic throttle valve system," *International Review of Applied Sciences and Engineering*, vol. 15, no. 1, pp. 107-115, 2024.

[58] C. E. Martínez Ochoa, I. O. Benítez González, A. O. Cepero Díaz, J. R. Nuñez-Alvarez, C. G. Miguélez-Machado, and Y. Llosas Albuerne, "Active disturbance rejection control for robot manipulator," *Journal of Robotics and Control (JRC)*, vol. 3, no. 5, pp. 622-632, 2022.

[59] N. A. Alawad, A. J. Humaidi, and A. S. Alaraji, "Observer sliding mode control design for lower exoskeleton system: Rehabilitation case," *Journal of Robotics and Control (JRC)*, vol. 3, no. 4, pp. 476-482, 2022.

[60] M. A. Mossa, H. Echeikh, and A. Ma'arif, "Dynamic Performance Analysis of a Five-Phase PMSM Drive Using Model Reference Adaptive System and Enhanced Sliding Mode Observer," *Journal of Robotics and Control (JRC)*, vol. 3, no. 3, pp. 289-308, 2022.